Effect of Carbon Black/Nanoclay Hybrid Filler on the Dynamic Properties of Natural Rubber Vulcanizates

Yuanbo Liu, Li Li, Qi Wang

State Key Laboratory of Polymer Materials Engineering, Polymer Research Institute, Sichuan University, Chengdu 610065, China

Received 29 November 2009; accepted 21 March 2010
DOI 10.1002/app.32486
Published online 28 May 2010 in Wiley InterScience (www.interscience.wiley.com).

ABSTRACT: In this study, natural rubber (NR) nanocomposites based on carbon black (CB) and two poly(ethylene glycol) (PEG)-modified clay hybrid filler were fabricated. The morphology and mechanical properties were studied. The dynamic properties of NR vulcanizates were investigated over a range of strain amplitude at two temperatures. It was found that NR with hybrid filler exhibits superior mechanical properties over that with CB as single phase filler. The hybrid filler causes a significant alteration in the dynamic properties of rubber. The Payne effect becomes more pronounced in rubber with modified clay. A decrease in loss factor (tanδ) was observed for rubber with hybrid filler also. The results revealed that the inclusion of nanoclay (NC) could induce a stronger and more developed filler network. Because of the anisotropy of the nanolayers, NC would depress the reconstruction of filler network, or lower the reformation rates when broken down under deformation, giving rise to lower tanδ value at broad temperature range as well as strain amplitude. © 2010 Wiley Periodicals, Inc. J Appl Polym Sci 118: 1111–1120, 2010

Key words: natural rubber; organoclay; nanocomposites; hybrid filler; dynamic properties

INTRODUCTION

Filled rubbers are used in a wide range of applications,[1] particularly in automotive tires, engine mounts, and vibration insulators. Reinforcing fillers play important roles in improving the mechanical properties of rubber matrix, including stiffness, strength, modulus, fatigue, and abrasion resistance.[2] Fillers are also the important elements to adjust the dynamic performances of rubber materials for specific applications via suitable choosing the filler.[3,4]

Reinforcement of rubber compounds dates back to 1904, when carbon black (CB) was used as nanofillers.[5] Also, in present days, CB is the principal reinforcement element for rubbers, along with silica.[6,7] However, there is a continuous demand for new, low-cost, low-weight, and environmental- friendly reinforcing filler in the rubber industry.[8,9] Extensive studies have been done on rubber/clay nanocomposites, showing that the stiff anisotropic nanoclay (NC) exhibits strong reinforcing effect in many rubber matrices, even at remarkably low clay content.[10–15] The unique properties imparted by NC and its potential to create new materials with superior properties have opened up a new prospect in developing CB/NC hybrid nanocomposites via partial replacement of CB with clay in rubber products without affecting the critical performance properties.

Because of the anisotropic nature of NC, the layers usually induce some unexpected structure in CB/NC-filled polymer systems, which is commonly considered to affect the macroscopic properties significantly. Several researches have shown that clay layers can bend around CB particles to form structure called "nanounit,"[16–18] resulting in improved properties. Differently, Etika et al.[19] have observed the formation of a unique "haloing" microstructure that clay layers are surrounded by CB particles, which subsequently enhances the electrical and mechanical performance of the nanocomposites. As rubber nanocomposites concerns, however, most published works are focused on the reinforcement mechanism of hybrid nanofiller in rubber[18,20]; little is known about its influence on the dynamic properties.

It is well known that CB particles in rubber matrix tend to agglomerate to form filler network at practical filling level. The filler network contributes a lot to the reinforcement,[21] and it is the main parameter governing the dynamic response of filled rubber.[22–25] The strength and architecture of the filler network are controlled by the amount, particle size, geometry, as well as surface chemistry of the filler. In a hybrid

Correspondence to: Q. Wang (qiwang@scu.edu.cn).
Contract grant sponsor: National Basic Research Program of China; contract grant number: 2007CB714700.

filler-rubber compound, the incorporation of clay nanolayers would influence the strength and architecture of the agglomerates structure of CB, thus change the mechanical as well as dynamic performance profoundly. So, studying the impact of CB/NC on the dynamic properties of rubber would have both applied and fundamental interest.[20]

In this work, we used two type of clay with distinct aspect ratio to exam the effect of hybrid CB/NC on the mechanical properties of CB-filled natural rubber (NR) vulcanizates with emphasis on the dynamic properties. Organic modification of the gallery surfaces of clay with poly(ethylene glycol) (PEG) compatibilizes them to the NR matrix, thus improves the dispersion and facilitates the intercalation or exfoliation of clay. It will be shown that dynamic properties of the NR vulcanizates are significantly affected by the hybrid filler.

EXPERIMENTAL

Materials

Natural rubber (CSR5) was provided by Yunnan Natural Rubber Industrial (Yunnan). Cloisite Na^+ (CNA), a Na^+-montmorillonite (Na^+MMT) clay, and Laponite RD (LRD), a synthetic hectorite-type clay, were purchased from Southern Clay Products (Gonzales, TX). Carbon black (N330) is a product of China Rubber Group Carbon Black Research & Design Institute (Zigong, Sichuan). Other additives used in the formulations are commercially available and was used as received.

Materials preparation

CNA and LRD were used as received without any further purification. The CNA and LRD clay platelets produce an opaque suspension and clear suspension in water, respectively. PEG with a molecular mass of 6000 kg/mol was used as received. For better dispersion of the clay platelets in the rubber matrix, the PEG-intercalated/exfoliated clay compounds were prepared by solution method. PEG and CNA or LRD were added to deionized water, followed by stirring for 4 days, centrifuging, and drying process. The organo-modified CNA and LRD are referred as OMMT and ORD, respectively.

Rubber compounds were prepared in an open two-roll mill at room temperature ($\sim$ 25°C). The rotors operated at a speed ratio of 1 : 1.4. Processing aids and rubber were first blended. Then clay, CB, and curatives were added orderly. The formulations of the compounds were compiled in Table I. The data in Table I are in parts per hundred parts of rubber (phr). All the samples contain the following curatives: 5.0 phr zinc oxide, 1.0 phr stearic acid, 2.3 phr sulfur, 1.0 phr MBTS (accelerator benzothiazyl disulfide), and 1.0 phr IPPD (antioxidant *N*-isopropyl-*N*′-phenyl-*p*-phenylenediamine). The samples were then cured at 150°C in an electrically heated hydraulic press to their respective cure times, t_{90}, which was derived from oscillating disk rheometer (R100E, Beijing Youshen Electronic Instrument) measurements.

Measurements and characterization

Wide angle X-ray diffraction

The dispersion of the clay was studied by WAXD. X-ray diffractograms were obtained using Ni-filtered Cu Kα radiation (λ = 0.1542 nm) by a DX-1000 diffractometer (Dandong Fangyuan Instrument, China) at 40 kV and 25 mA. The samples were scanned in step mode by 0.06/s scan rate in the range of 2Θ = 2–40°.

Differential scanning calorimetry

The thermal properties of nanocomposites were measured using Q20 instrument (TA), previously calibrated with aluminum. First, all samples were cooled to −80°C and then heated to 160°C for 5 min. Then, the second scanning of heating and cooling run was also performed between −80°C and 160°C. The whole process was carried out at a rate of 10°C/min.

Transmission electron microscopy and scanning electron microscopy

The dispersion and morphology of the clay nanoparticles in the rubber matrix were observed through TEM, using a Hitachi H-600 TEM operated at an accelerating voltage of 100 kV. TEM samples with $\sim$ 100 nm thickness were prepared by sectioning at −160°C using a cryoultramicrotome with a diamond knife.

Samples with 2 mm thickness were cryo-fractured and the fractured surfaces were observed after spraying a thin gold layer, with a scanning electron microscope (INSPECT F, FEI, Japan) under an accelerating voltage of 5 kV.

Static mechanical properties

Tensile and tear tests were performed at room temperature on an Instron universal testing machine (INSTRON 5567) with a cross-head speed of 500 mm/min. The dumbbell and angle shaped specimens were prepared according to the ISO standards ISO 37 and ISO 34. Five specimens were tested and the average was taken. Hardness was tested using a hardness meter according to ASTM 2240.

TABLE I
List of the Compounds Ingredient

Samples	NR (SCR)	CB (N330)	CNA	LRD	OMMT	ORD
NR	100					
NR/CNA	100		10			
NR/LRD	100			10		
NR/OMMT	100				10	
NR/ORD	100					10
NR/CB	100	25				
NR/CB/CNA	100	25	5			
NR/CB/LRD	100	25		5		
NR/CB/OMMT	100	25			5	
NR/CB/ORD	100	25				5

Dynamic mechanical analysis

The dynamic properties of the vulcanizates were measured by means of a dynamic mechanical analyzer (TA Q800) using strip specimens with size (length × width × thickness) 15 × 5 × 2 mm^3 operated in the tensile mode. Two type of tests, namely temperature sweeps and strain sweeps, were performed. The temperature sweeps measurement was carried out at a strain of 0.02%. Storage and loss moduli and mechanical loss factor (tanδ) were recorded in the temperature range from −100 to 60°C at a heating rate of 3°C/min. The frequency used was 1.0 Hz. In the case of strain sweeps, strain amplitudes ranging from 0.1 to 20% were applied with a frequency of 10 Hz at constant temperature of −20°C and 60°C, respectively.

RESULTS AND DISCUSSIONS

Dispersion state of clay and CB in NR

The prerequisite for reinforcing rubber is the good dispersion of filler. Therefore, it is necessary to investigate the dispersion state of clay and CB in rubber first. From the WAXD curves shown in Figure 1, it is clearly seen that the 001 diffraction peak of CNA shifts originally from $2\Theta = 7.5°$ to about 5° after modification with PEG, suggesting that the *d*-spacing was enlarged from 1.17 nm to 1.79 nm. When the modified MMT was incorporated into NR, the peak is no longer varied, indicating that intercalated structure of MMT was formed and preserved after compounding with NR. Similar diffraction peak evolution can be found with LRD, where the *d*-spacing increases from 1.20 to 1.84 nm. The WAXD results show that PEG can behave as swelling agent, favoring the diffusion of NR chains into the clay galleries, which is in accordance with that in literature.[26]

Carretero-González[26] and Evans[27] found that *d*-spacing of Na^+MMT would reach a maximum of about 18 Å when modified with over 19 wt % PEG, independently of the polymer molecular weight and processing method. Different from organoclay prepared through ion-exchanging by commonly used quaternary ammonium salt, PEG-modified clay usually allows rubber chains located far away from the

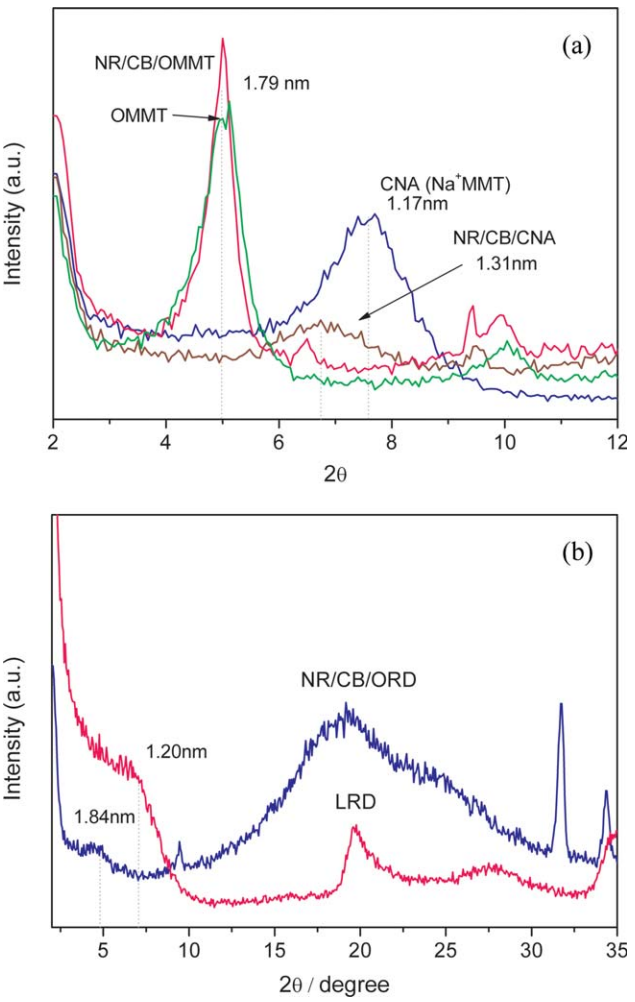

Figure 1 WAXD patterns of (a) CNA and (b) LRD and their PEG-modified counterparts in natural rubber. [Color figure can be viewed in the online issue, which is available at www.interscience.wiley.com.]

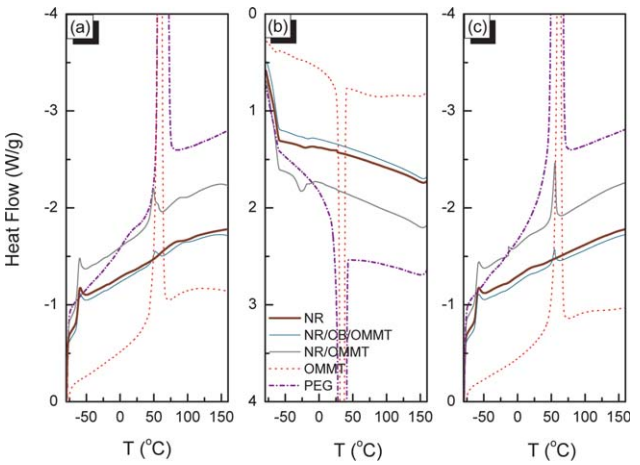

Figure 2 DSC curves for (a) heat, (b) cool, (c) second heat cycles corresponding to the PEG, OMMT, NR/OMMT, NR/CB/OMMT, and unfilled NR samples as indicated. [Color figure can be viewed in the online issue, which is available at www.interscience.wiley.com.]

silicate surface interacting with PEG chains, whereas the PEG chains are acting as interface between the most hydrophobic component in the gallery, as a scenario proposed literature.[26] Hence, the MMT are intercalated by NR as well as PEG chains. In the case of ORD, the 001 peak is much weak than that of OMMT [Fig. 1(b)], which can be assumed that most clay layers were exfoliated in the rubber matrix during compounding due to their smaller clay size (25–30 nm).[28]

With the DSC results displayed in Figures 2 and 3, the morphology of organo-modified clay in rubber can be better understood from their different thermal behaviors during heating or cooling.[8]

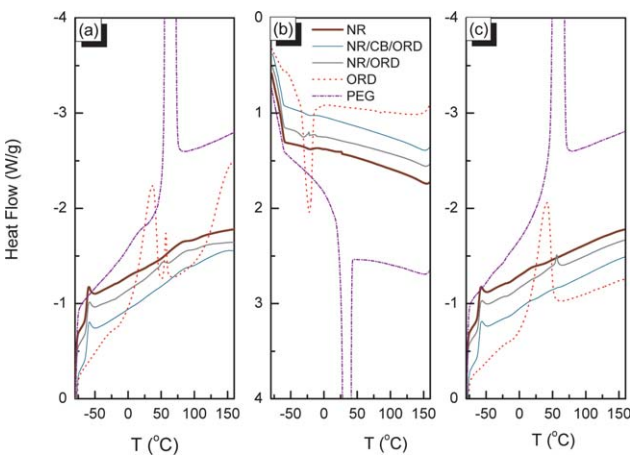

Figure 3 DSC curves for (a) heat, (b) cool, (c) second heat cycles corresponding to the PEG, ORD, NR/ORD, NR/CB/ORD, and unfilled NR samples as indicated. [Color figure can be viewed in the online issue, which is available at www.interscience.wiley.com.]

In the first heating cycle, PEG and OMMT exhibit intense endothermic peak at 65°C and 60°C, respectively, corresponding to the melting transition of PEG chains [Fig. 3(a)]. An obvious shift of this endothermic peak can be observed in NR/OMMT as well as NR/CB/OMMT, where the transition temperature decreases to 50°C and 52°C, respectively. During the second heating, the shift of melting transition of PEG in the compounds is more clearly displayed, which decreases from 61°C for PEG and 63°C for OMMT to 56°C for NR/OMMT and 55°C for NR/CB/OMMT. This transition can be attributed to the conformational changes of PEG packed in the gallery and the variations of molecular environment due to polymer intercalation.[8] In contrast, the melting transition of PEG almost disappears in Figure 3 for NR/ORD and NR/CB/ORD, both in initial and second heating cycles, indicating that no packed PEG chains as well as confined NR chains exist. The reason for this should be that ORD was highly dispersed and exfoliated. Therefore, DSC results support the evidence from WAXD that intercalated and exfoliated morphology predominates in OMMT and ORD-filled

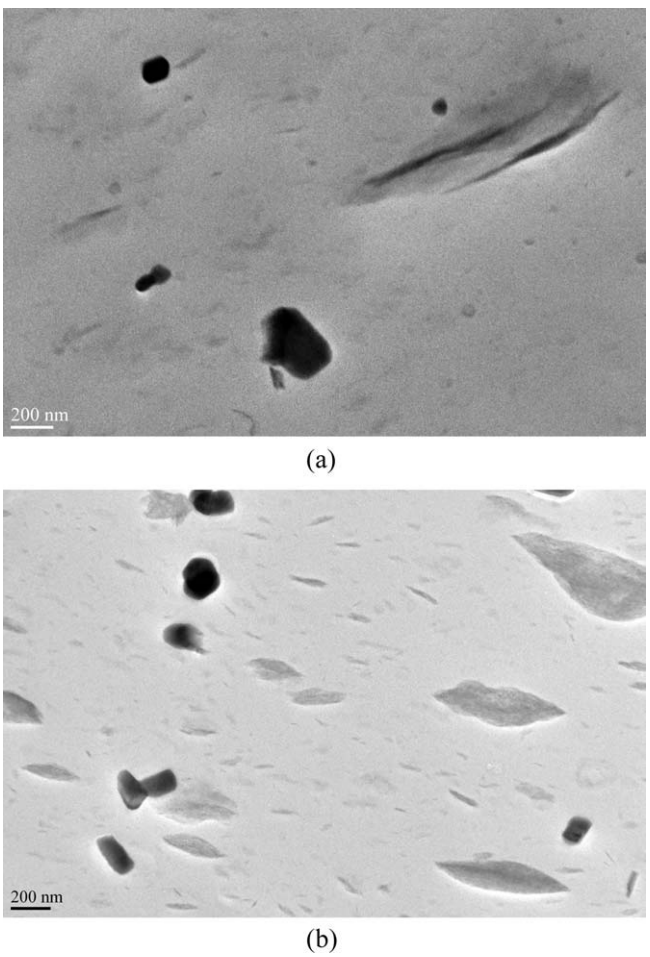

Figure 4 TEM micrographs of (a) NR/OMMT and (b) NR/ORD.

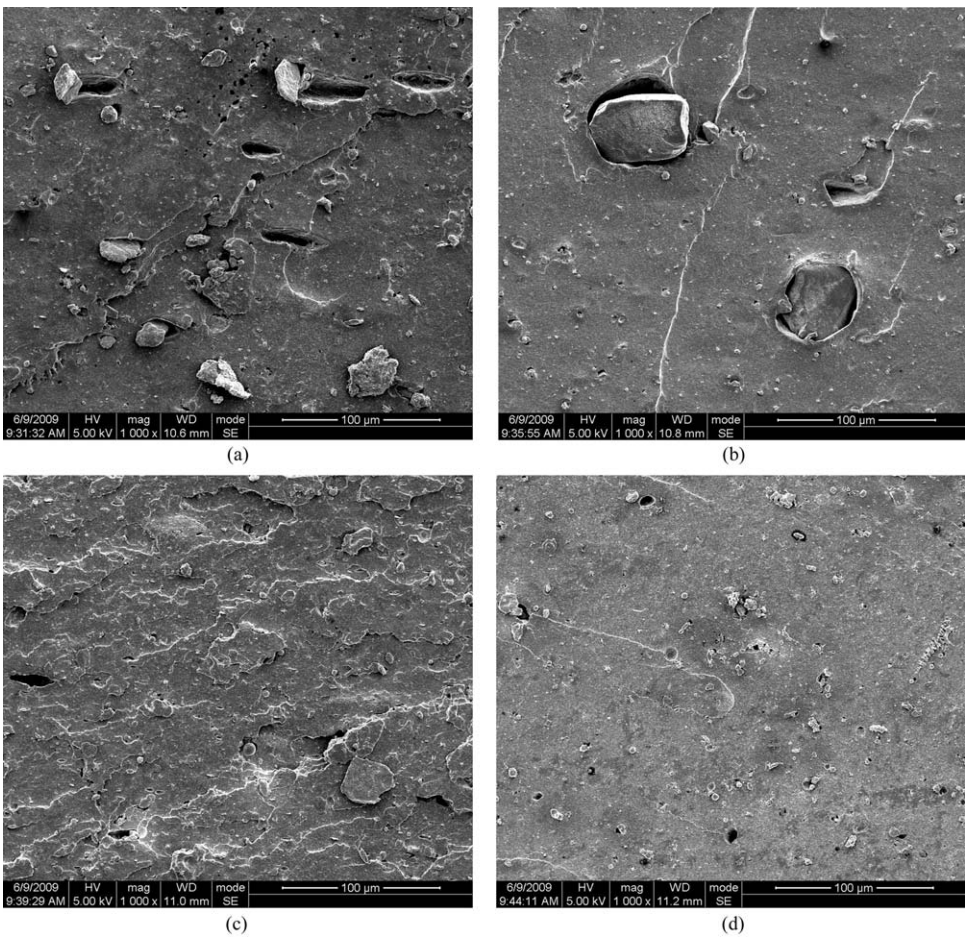

Figure 5 SEM micrographs showing tensile fracture surface of (a) NR/CB/CNA, (b) NR/CB/LRD, (c) NR/CB/OMMT, and (d) NR/CB/ORD.

NR, respectively, as confirmed by TEM micrographs shown in Figure 4.

Finally, it should be pointed out that the presence of the broad and nonreversible endothermic transition at about 100°C during initial heating [Fig. 3(a)] of almost all the samples reflects the release of physically absorbed water. Vulcanized NR materials exhibit a near constant secondary transition at −60°C, corresponding to the glass transition temperature of the polymer network.

Figure 5 displays the SEM micrographs taken from the tensile fracture surfaces of NR composites. It is clearly shown that there are number of large particles in NR/CB/CNA and NR/CB/LRD, which are the agglomerates of unmodified CNA [Fig. 5(a)] and LRD [Fig. 5(b)]. It is believed that pristine clay, both for CNA and LRD, can not be wetted by the polymer chains due to their hydrophilic nature surface. As discussed before, OMMT and ORD are intercalated with PEG chain, which facilitates the diffusion and wetting of rubber chains. The shear force is sufficient to break down the clay agglomerates during compounding, resulting in the improved dispersion.

Effect of the NC/CB hybrid filler on the mechanical properties of NR vulcanizates

Figure 6 is the stress–strain curve of NR materials. The data for mechanical properties are compiled in Table II in detail. It can be seen that both the modulus at given elongations and the maximum tensile strength of NR/CB/OMMT and NR/CB/ORD are considerably higher than their microcomposites counterparts, i.e., NR/CB/CNA and NR/CB/LRD, as well as NR/CB. However, without CB, the organoclay-reinforced NR vulcanizates exhibit only improved strength, with limited enhancement in modulus, as displayed in Figure 6(b). The enhancement in tensile strength should be attributed to the improved interfacial interaction between the clay layers and rubber benefited from the organic modification, which may improve the strain-induced crystallization of NR. The increase of elongation at break of NR/OMMT and NR/ORD may be attributed to the better dispersed clay layers in NR matrix, with which the rubber can endure larger deformation without rupture. As concerns the modulus at small elongation, it is related to the filler network. In the hybrid-filled nanocomposites, OMMT and ORD are both anisotropic fillers,

which easily form dual phase network with CB aggregates in such a highly jammed system. A portion of the rubber is entrapped in the filler network as "dead" rubber. This part of rubber could be shielded from deformation, acting as rigid filler. From this point of view, the enhancement in tensile behavior of the nanocomposites can be reasonably interpreted. Besides tensile property, tear strength and hardness of NR rubber are also largely improved by filling with CB and NC. The mechanical properties tests reveal that CB and NC have a good synergistic reinforcing effect on NR.

Effect of the NC/CB hybrid filler on the dynamic properties of NR vulcanizates

Temperature sweeps

Figure 7 shows the variation of storage modulus (G') and the loss factor (tanδ) as a function of

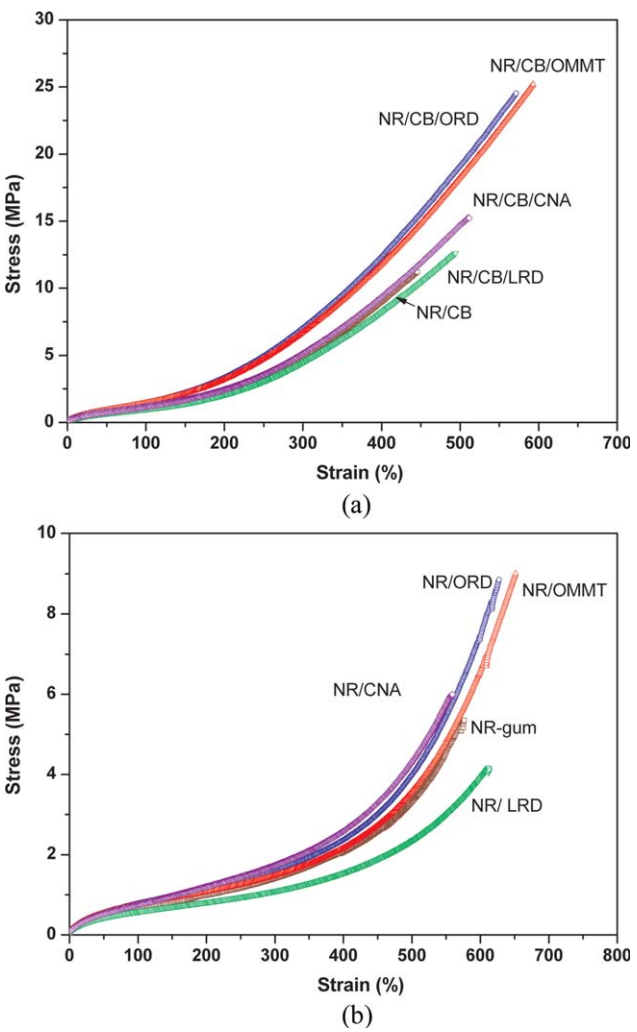

Figure 6 Stress–strain curves of (a) NR/CB, NR/CB/Clay composites and (b) NR gum, NR/Clay composites. [Color figure can be viewed in the online issue, which is available at www.interscience.wiley.com.]

TABLE II
Mechanical Properties of NR Gum and Filled NR Vulcanizates

	NR	NR/CNA	NR/LRD	NR/OMMT	NR/ORD	NR/CB	NR/CB/CNA	NR/CB/LRD	NR/CB/OMMT	NR/CB/ORD
Maximum strength (MPa)	5.1	5.9	4.1	8.8	8.8	11.3	14.5	12.8	25.4	24.5
Elongation at break (%)	572	554	603	655	624	460	524	480	605	565
100% Modulus (MPa)	0.65	0.76	0.59	0.72	0.79	0.95	1.11	1.05	1.43	1.51
200% Modulus (MPa)	0.96	1.21	0.83	1.03	1.16	2.07	2.25	2.22	3.14	3.46
300% Modulus (MPa)	1.38	1.74	1.11	1.41	1.61	4.59	4.63	4.85	6.59	7.31
Tear Strength (kN/m)	20.0	19.9	15.5	20.3	22.7	25.2	25.5	25.2	33.6	33.6
Hardness (Shore A)	31	33	28	33	35	37	41	39	46	47

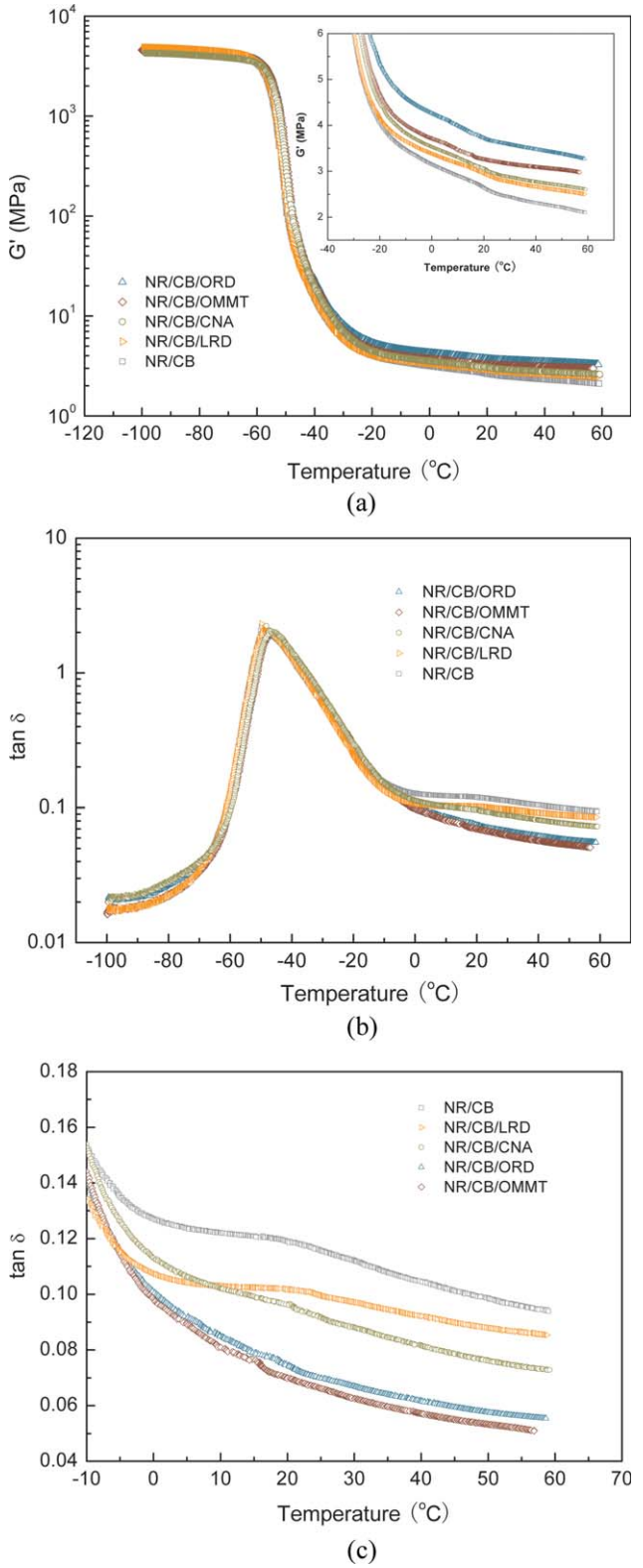

Figure 7 Temperature dependence of G' (a) and tanδ (b and c) for NR compounds with indicated fillers. [Color figure can be viewed in the online issue, which is available at www.interscience.wiley.com.]

temperature for the rubber materials. At low temperature, the polymer is in the glassy state with a modulus around 40 GPa. With increasing temperature, the elastic moduli suddenly drop down by 3 orders of magnitude corresponding to the glass–rubber transition, which is in accordance with other researches.[8,29] This modulus drop can be ascribed to an energy dissipatation phenomenon involving cooperative motions of long chain sequences.

Compared with CB-filled rubber, G' increases significantly for hybrid-filled composites in the rubbery zone; little G' improvement in the glassy state is observed. For CB-filled rubber, the increase observed in the rubbery region is generally resulted from the agglomeration and filler networking of CB. In a hybrid system similar with ours, NC/silica, Schon et al.[25] suggested that when the filler particles or aggregates get into contact and are able to build up a filler network, the modulus increase is much stronger. So, it is reasonable to ascribe the G' increase here to the filler networking of the hybrid filler. In addition, it is of interest to note the loss factor variation of the composites, which was shown in Figure 7(b,c). No obvious change in the peak of tanδ can be observed in the transition zone. Whereas, the tanδ is profoundly varied in the temperature ranging from 0°C to 60°C. The hybrid filler with OMMT and ORD gives much lower tanδ value as compared with other three one. The reason for this will be discussed later.

Strain sweeps

The strain dependence of G' at 60°C and −20°C is shown in Figure 8. As can be seen, the modulus of the NR gum does not change significantly upon increasing strain amplitude over the range tested. However, it decreases for all the filled samples with growing strain. This nonlinear behavior is known as Payne effect.[3] For CB-filled vulcanizates, it has been widely accepted that the Payne effect is mainly related to the filler network.[22,30] Payne effect is exponentially increased by increasing filler loading. NR/CB/OMMT and NR/CB/ORD show higher modulus at low strain amplitude and more obvious Payne effect at both temperatures as compared with other samples. This would be an indication of a more developed and stronger filler network.

As mentioned in the former section, filler network provides additional reinforcement by trapping rubber, thus increases the effective volume fraction of the filler. The collapse or breakdown of filler network with increasing strain would release the trapped rubber so that more rubber can take part in the strain process and the modulus decreases. This suggests that the Payne effect can be used to measure filler networking, which originates from filler–filler interaction as well as filler–rubber interaction.

Further, many studies have pointed out that filler network can be visualized by filler–filler contacts or

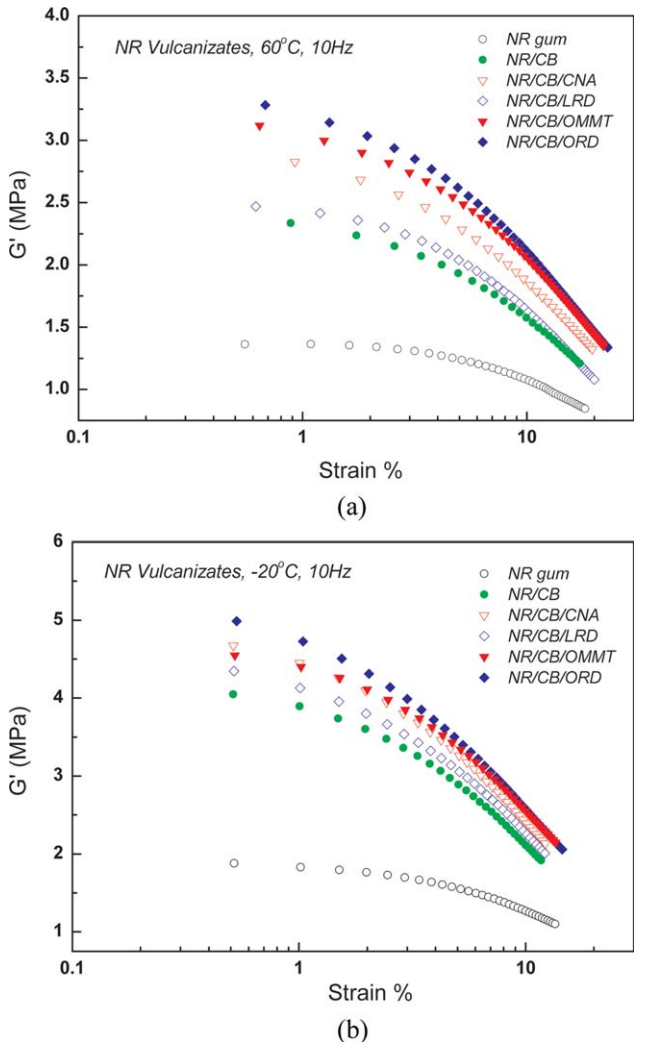

Figure 8 Strain dependence of G' at (a) 60°C and (b) −20°C and 10 Hz for NR compounds with indicated fillers. [Color figure can be viewed in the online issue, which is available at www.interscience.wiley.com.]

via a layer of immobilized rubber on the filler surface,[14,31] if so, Payne effect would have temperature dependence along with the strain dependence. In Figure 8(b), the strain sweeps were performed at −20°C, at which the rubber matrix is still in the transition zone. All the composites show higher modulus level than the modulus measured at 60°C at the same strain amplitude. However, the G' of NR/CB/ORD and NR/CB/OMMT get more close to NR/CB, showing that the hybrid filler network is easy to be broken down at lower temperature due to the more brittle polymer matrix.

The strain dependence of the loss modulus (G'') of vulcanizates with and without fillers is presented in Figure 9 at 60 and −20°C. Evidently, the incorporation of fillers in NR substantially increases the G'' of vulcanizates regardless of the strain amplitude. G'' would increase with increasing filler loading due to the hydrodynamical effect.[32] It is interesting to note that filled composites exhibit distinct G'' enhancement as compared with gum rubber. Unlike the composites containing unmodified clay, which shows an improvement on NR/CB, the hybrid nanocomposites with modified clay show lower G''. Because G' is mainly related to filler network which subsists during dynamic strain, and G'' is related to the breakdown and reformation of these structure.[30] The above result suggests that less filler network will be broken down and reformed during dynamic strain with CB/OMMT and CB/ORD. The higher G' and lower G'' with CB/NC hybrid can lead to a reasonable conclusion that the nanolayers of clay are inclining to depress the reconstruction, or to lower the reformation rates of filler network. The reason behind is the reduced mobility and hindered free rotation of clay tactoids[33] by the adjacent clay layers or the CB aggregates due to its anisotropy, which

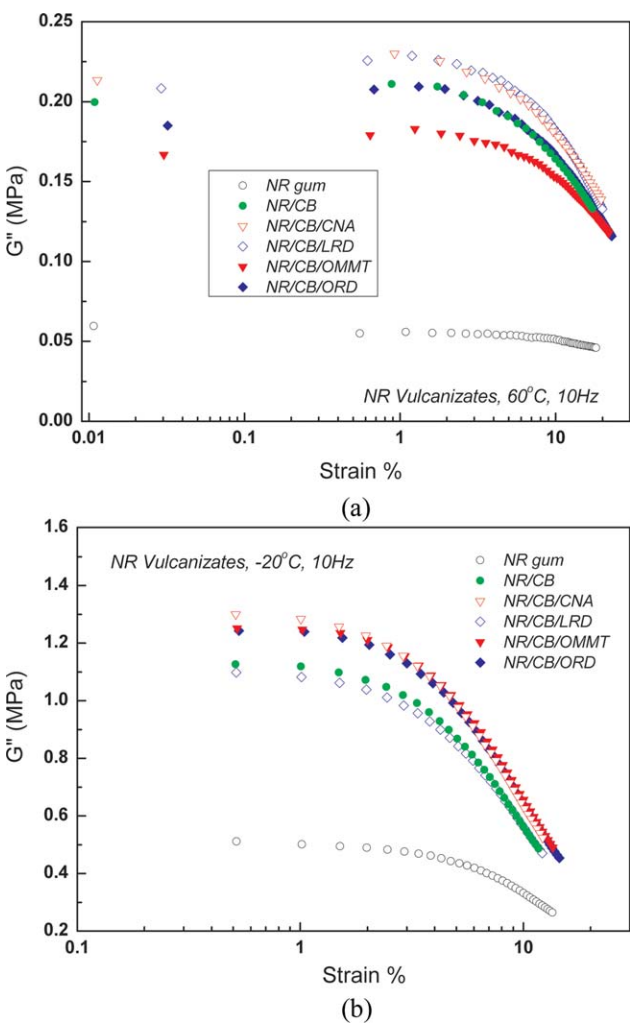

Figure 9 Strain dependence of G'' at (a) 60°C and (b) −20°C and 10 Hz for NR compounds with indicated fillers. [Color figure can be viewed in the online issue, which is available at www.interscience.wiley.com.]

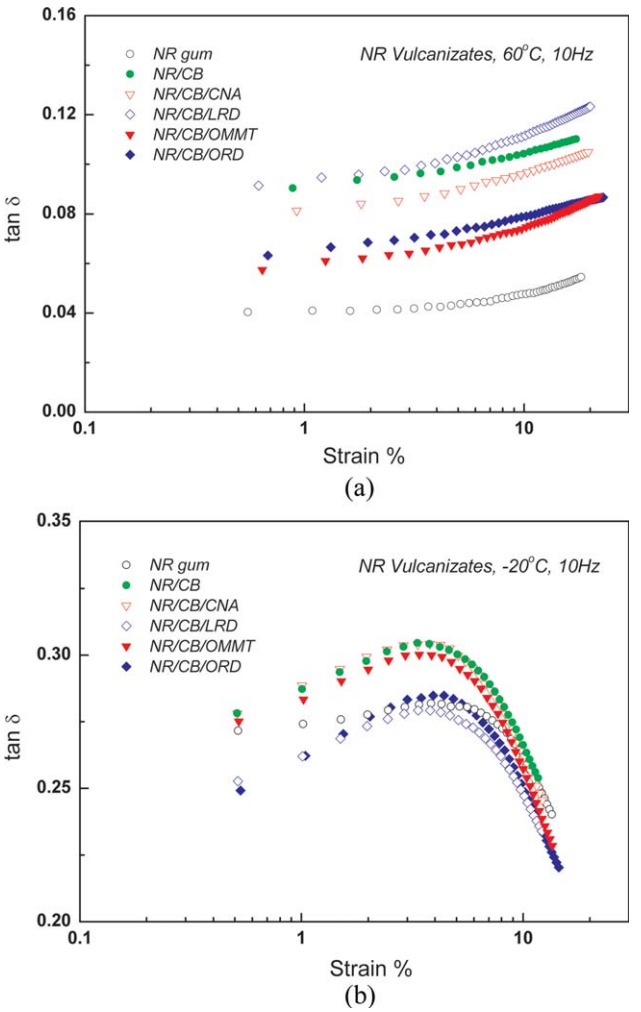

Figure 10 Strain dependence of tanδ at (a) 60°C and (b) −20°C and 10 Hz for NR compounds with indicated fillers. [Color figure can be viewed in the online issue, which is available at www.interscience.wiley.com.]

makes the layers easy to orientate along the force direction applied under deformation.

At −20°C, G'' of the filled rubber is mainly controlled by the rubber matrix, in which the internal friction between the polymer chains as well as between the polymer chains and the fillers determines the energy dissipating. Therefore, the loss modulus of NR/CB/OMMT and NR/CB/ORD is comparable to the CB-filled vulcanizates.

The loss factor is a ratio of G'' to G', which is representative of work converted into heat to that recovered, for a given work input during dynamic strain. Many mechanisms will influence tanδ. For filled rubber, the factor predominantly determining tanδ is the state of filler-related structures, or more precisely, the ratio between the portion capable of being broken down and reconstituted and those remaining unchanged during deformations.[22] So, it can be deduced that a more developed filler network with decreased reformation rate under deformation would give rise to a lower tanδ. It can be seen in Figure 10; the hybrid vulcanizates with OMMT and ORD have much lower tanδ than other filled samples at 60°C.

At relatively high temperature, the main cause of energy dissipation is related to the change of filler network structure because the polymer is in rubbery state with very high entropic elasticity. Although at low temperature that fall in the transition zone of the polymer, the hysteresis of the polymer needs to be taken into consideration. The energy loss is high due to its high viscosity, hence, longer relaxation time of rubber matrix. For the filled rubber, under small strain amplitude that the filler network can not be broken down, the polymer fraction will be reduced so that the loss factor would be lower. As can be seen in Figure 10(b), almost all the filled samples exhibit lower loss than the gum rubber. Whereas at higher strain, increase in loss factor of filled rubbers is observed because of the breaking down of the filler rubber, and that the friction between polymer chains and the filler surface will contribute to this increase.

CONCLUSIONS

The hybrid CB/NC-filled NR nanocomposites were prepared in the presence of two PEG-modified organoclay by melt mixing. Intercalated and exfoliated structure is dominated in OMMT and ORD-filled rubber, respectively, as revealed by WAXD and DSC.

Tensile tests and dynamic mechanical analysis display that the two phase fillers have significant synergistic reinforcing effect on natural rubber, which is believed to be originated from the filler network. Dynamic properties investigation of the rubber materials confirms the filler network and further indicates that the inclusion of NC layers, both OMMT and ORD, leads to a more developed network. The anisotropy of the clay makes it depress the reconstruction and to some extent lower the reformation rate of the filler network. So, decreased loss factor is observed in CB/NC-filled natural rubber. This characteristic may make CB/NC hybrid filler of interest in the applications that low hysteresis is preferred.

The authors are grateful to Prof. Dr. Robert M. Briber and Dr. Xin Zhang, Department of Materials Science and Engineering, University of Maryland, for the TEM characterization.

References

1. Gent, A. N., Ed. Engineering with Rubber—How to Design Rubber Components; Hanser: Munich, 2001.

2. Voet, A. J Polym Sci Macromol Rev 1980, 15, 327.
3. Payne, A. R. J Appl Polym Sci 1962, 6, 57.
4. Ramier, J.; Gauthier, C.; Chazeau, L.; Stelandreand, L.; Guy, L. J Polym Sci Part B: Polym Phys 2007, 45, 286.
5. Mohammadand, A.; Simon, G. P. Rubber-Clay Nanocomposites; Woodhead Publishing Limited, CRC Press: Cambridge, 2006.
6. Botti, A.; Pyckhout-Hintzen, W.; Richter, D.; Urbanand, V.; Straube, E. J Chem Phys 2006, 124, 174908.
7. Meera, A. P.; Said, S.; Grohensand, Y.; Thomas, S. J Phys Chem C 2009, 113, 17997.
8. Carretero-Gonzalez, J.; Retsos, H.; Verdejo, R.; Toki, S.; Hsiao, B. S.; Giannelisand, E. P.; Lopez-Manchado, M. A. Macromolecules 2008, 41, 6763.
9. Di Gianni, A.; Colucci, G.; Priola, A.; Conzatti, L.; Alessiand, M.; Stagnaro, P. Macromol Mater Eng 2009, 294, 705.
10. Arroyo, M.; Lopez-Manchadoand, M. A.; Herrero, B. Polymer 2003, 44, 2447.
11. Lebaronand, P. C.; Pinnavaia, T. J. Chem Mater 2001, 13, 3760.
12. Wangand, Z.; Pinnavaia, T. J. Chem Mater 1998, 10, 3769.
13. Sengupta, R.; Chakraborty, S.; Bandyopadhyay, S.; Dasgupta, S.; Mukhopadhyay, R.; Auddyand, K.; Deuri, A. S. Polym Eng Sci 2007, 47, 1956.
14. Ramorino, G.; Bignotti, F.; Pandiniand, S.; Ricco, T. Compos Sci Technol 2009, 69, 1206.
15. Pramanik, M.; Srivastava, S. K.; Samantarayand, B. K.; Bhowmick, A. K. J Appl Polym Sci 2003, 87, 2216.
16. Konishiand, Y.; Cakmak, A. Polymer 2006, 47, 5371.
17. Praveen, S.; Chattopadhyay, P. K.; Albert, P.; Dalvi, V. G.; Chakrabortyand, B. C.; Chattopadhyay, S. Compos Part A: Appl Sci Manuf 2009, 40, 309.
18. Chattopadhyay, P. K.; Basuliand, U.; Chattopadhyay, S. Polym Compos 2009; Doi: 10.1002/pc.20866.
19. Etika, K. C.; Liu, L.; Hessand, L. A.; Grunlan, J. C. Carbon 2009, 47, 3128.
20. Jia, Q. X.; Wu, Y. P.; Xiang, P.; Ye, X.; Wangand, Y. Q.; Zhang, L. Q. Polym Polym Compos 2005, 13, 709.
21. Peng, C. C.; Gopfert, A.; Drechslerand, M.; Abetz, V. Polym Adv Technol 2005, 16, 770.
22. Wang, M. J. Rubber Chem Technol 1999, 72, 430.
23. Bokobza, L. Macromol Mater Eng 2004, 289, 607.
24. Kluppel, M. Macromol Mater Eng 2009, 294, 130.
25. Schonand, F.; Gronski, W. Kautsch Gummi Kunstst 2003, 56, 166.
26. Carretero-Gonzalez, J.; Valentin, J. L.; Arroyo, M.; Saalwachterand, K.; Lopez-Manchado, M. A. Eur Polym J 2008, 44, 3493.
27. Chenand, B. Q.; Evans, J. R. G. Polym Int 2005, 54, 807.
28. Stefanescu, E. A.; Dalyand, W. H.; Negulescu, I. I. Macromol Mater Eng 2008, 293, 651.
29. Sadhuand, S.; Bhowmick, A. K. Rubber Chem Technol 2005, 78, 321.
30. Heinrichand, G.; Klüppel, M. Advances in Polymer Science; Springer: Berlin/Heidelberg, 2002; 1.
31. Ouyang, G. B. Kgk-Kautschuk Gummi Kunstst 2006, 59, 332.
32. Wang, M. J. Rubber Chem Technol 1998, 71, 520.
33. Wang, K.; Liang, S.; Deng, J. N.; Yang, H.; Zhang, Q.; Fu, Q.; Dong, X.; Wangand, D. J.; Han, C. C. Polymer 2006, 47, 7131.